Front. Phys. 11(4), 114209 (2016)
DOI 10.1007/s11467-016-0581-6

RESEARCH ARTICLE

The role of microwaves in the enhancement of laser-induced plasma emission

Ali Khumaeni[1,†], Katsuaki Akaoka[2], Masabumi Miyabe[2], Ikuo Wakaida[2]

[1] *Department of Physics, Faculty of Science and Mathematics, Diponegoro University, Tembalang, Semarang 50275, Indonesia*
[2] *Fuel Debris Analysis Group, Collaborative Laboratories for Advanced Decommissioning Science (CLADS), Japan Atomic Energy Agency, Tokai-mura, Ibaraki-ken 311-1195, Japan*
Corresponding author. E-mail: †khumaeni@fisika.undip.ac.id
Received November 13, 2015; accepted February 20, 2016

We studied experimentally the effect of microwaves (MWs) on the enhancement of plasma emission achieved by laser-induced breakdown spectroscopy (LIBS). A laser plasma was generated on a calcium oxide pellet by a Nd:YAG laser (5 mJ, 532 nm, 8 ns) in reduced-pressure argon surrounding gas. A MW radiation (400 W) was injected into the laser plasma via a loop antenna placed immediately above the laser plasma to enhance the plasma emission. The results confirmed that when the electromagnetic field was introduced into the laser plasma region by the MWs, the lifetime of the plasma was extended from 50 to 500 μs, similar to the MW duration. Furthermore, the plasma temperature and electron density increased to approximately 10900 K and 1.5×10^{18} cm^{-3}, respectively and the size of the plasma emission was extended to 15 mm in diameter. As a result, the emission intensity of Ca lines obtained using LIBS with MWs was enhanced by approximately 200 times compared to the case of LIBS without MWs.

Keywords laser-induced breakdown spectroscopy, LIBS, microwave-assisted laser-induced breakdown spectroscopy, MA-LIBS, enhancement of laser plasma emission

PACS numbers 42.62.Fi, 95.75.Fg, 42.55.-f, 42.62.-b, 87.50.S-

1 Introduction

Laser-induced breakdown spectroscopy (LIBS) is one of the most powerful analytical methods for spectrochemical analysis. In LIBS, a Nd:YAG laser is usually focused onto a sample target to generate a luminous plasma [1, 2]. The elemental composition of the target can be obtained by analyzing the atomic emission from the plasma. The appealing advantages of LIBS are the use of unprocessed samples, the possibility of in-situ analysis, and the capability of micro-area analysis [3]. For these reasons, LIBS has been successfully implemented for elemental analysis in various fields, such as the environmental field [4, 5], the metal industries [6–8], and nuclear power plants [9]. LIBS has also been used for calcium detection; calcium analysis is known to be necessary in various applications, including soil analysis, the coal industry, and environmental. Bustamante *et al.* performed Ca analysis in soil using LIBS [10]. Maravelaki-Kalaitzaki *et al.* employed LIBS for the characterization of encrustation on marble [11]. Body and Chadwick conducted research on coal analysis using LIBS [12]. Although LIBS has numerous applications, it suffers from reduced sensitivity compared to other spectroscopic methods.

To overcome this drawback, efforts have been made by many LIBS groups to develop the double-pulse LIBS technique (DP-LIBS) [13–15], which can be effectively used for the improvement of the analytical capabilities of single-pulse LIBS (SP-LIBS). DP-LIBS obtains significant increases in the signal-to-noise ratio (S/N) and the emission intensity compared to SP-LIBS. The enhancement in line emission intensity achieved by double-pulse excitation is believed to be due to the increased ablated mass, higher plasma temperature, and longer plasma duration [16].

Other methods aimed at enhancing the emission intensity have been developed by coupling microwave (MW) and laser systems, which is known as MW-assisted LIBS (MA-LIBS). Envimetrics and Liu *et al.* used MWs to enhance the plasma emission of metal samples [17, 18]. Kearton *et al.* and Liu *et al.* reported intensity enhance-

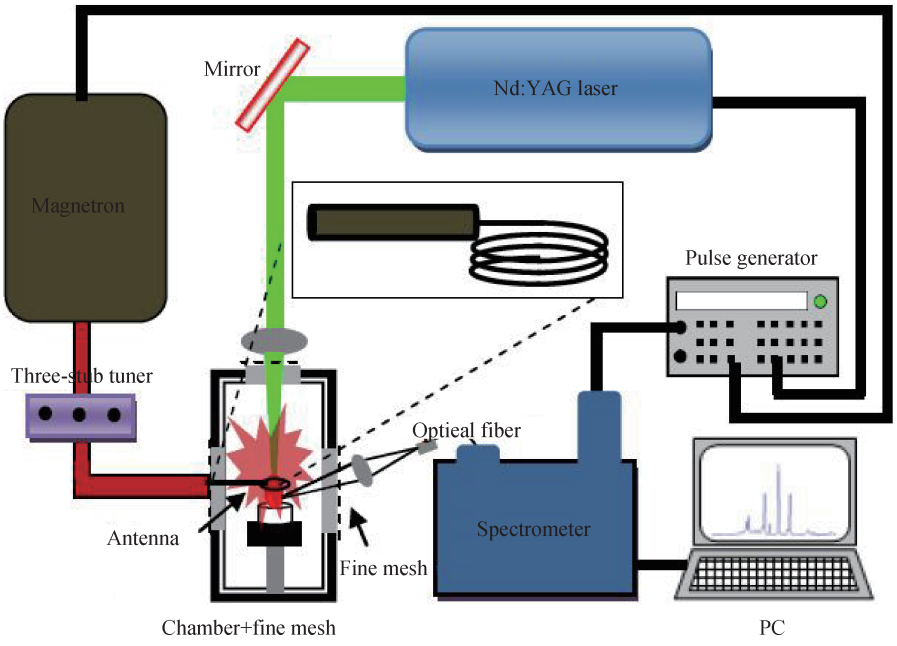

Fig. 1 Experimental setup used in this work.

ments obtained by using laser-assisted MW spectroscopy (LAMPS) [19, 20]. Ikeda *et al.* used MWs to extend the lifetime of plasma emission to the order of a millisecond [21]. However, these methods required the use of waveguides and microwave cavities.

For the convenient application of MWs, we developed a method of MA-LIBS coupled with a loop antenna for the enhancement of LIBS emission. In this method, a luminous plasma is generated by a low-energy pulsed laser at a local point, where an electromagnetic field is produced by localized MW radiation. The MWs are applied through a loop antenna via a coaxial cable to enhance the plasma emission. We must emphasize that this method is especially suitable for practical application because the antenna is very flexible and can access the sample via the coaxial cable, which is combined with a fiber system. Thus, the technique is highly applicable to material analysis in the field. In contrast, previously proposed MA-LIBS methods required waveguides and microwave cavities, which is inconvenient for practical applications because the sample must be placed in a special chamber connected to the MW source.

In this study, the effect of MWs on the enhancement of laser plasma emission was studied by measuring time-resolved emission spectra obtained with (MA-LIBS) and without MWs (LIBS). Pelletized calcium oxide (CaO) powder was used as the sample.

2 Experimental setup

The basic experimental setup used in this work is shown in Fig. 1. A Q-switched Nd:YAG laser (Quanta-Ray, Spectra Physics, 532 nm, 8 ns) was directly focused onto a sample surface through a quartz window (200 mm) to generate a plasma. The laser energy was fixed at 5 mJ. The plasma emission was enhanced by intensified MWs produced via a loop antenna; the antenna was shaped as a loop with a diameter of 3 mm. MWs were generated using a magnetron at a frequency of 2.45 GHz (MUEGGE MG0500D-215TC, 400 W, 0–1 ms). The MW impedance could be experimentally adjusted for the plasma generation by a three-stub tuner. The Nd:YAG laser and MWs were operated in the synchronization mode and a delay time of 10 μs was used for the Nd:YAG laser bombardment relatively to the MW generation to obtain MWs with good stability.

The sample used in the study was a calcium oxide (CaO) pellet, which has relatively simple spectral lines. During the experiment, the sample was placed in a metal chamber equipped with windows, on which a fine-plated gold mesh (lattice constant of 80 μm and wire diameter of 30 μm) was attached. The experiment was performed in reduced-pressure Ar surrounding gas (0.6 kPa).

The emission spectrum was obtained by using an intensified charge-coupled device (ICCD) camera (Andor, iStar) through a high-resolution echelle spectrometer (LTB ARYELLE) with a resolution of 50 pm. The light emission of the laser plasma was collected by an optical fiber positioned at approximately 80° relatively to the laser axis (Fig. 1). The plasma radiation from the sample surface for the LIBS and MA-LIBS cases was imaged at one end of the fiber using a quartz lens ($f = 100$ mm). To study the dynamics of plasma expansion, an ICCD

camera (Andor, iStar) was used. The plasma emission was imaged by using a quartz lens placed in the ICCD.

3 Results and discussion

To determine the optimum emission intensity of Ca lines in laser-induced plasma with and without MWs, the spatial distribution of the time-integrated emission intensity of Ca was measured. Figure 2 displays the emission intensities of Ca II 393.3 nm and Ca I 422.6 nm, measured perpendicularly to the sample surface. The figure shows that the time-integrated emissions of Ca II and Ca I are distributed up to 10 mm and 5 mm from the sample surface in the case of MA-LIBS and LIBS, respectively. In the MA-LIBS case, the optimum emission intensity of Ca ions was located at 4 mm to 7 mm from the sample surface, and in the case of LIBS, at 2 mm. It must be mentioned that the position of the loop antenna was 3 mm above the sample surface. In the experiment, the laser beam was focused on the sample surface after passing through the inner side of the antenna. It is assumed that the optimum intensity was obtained at 4 to 7 mm because the electromagnetic field was optimum in the interior of the loop antenna. Based on this result, we used 5 mm and 2 mm heights from the sample surface for the data acquisition in MA-LIBS and LIBS, respectively.

Figure 3 shows the emission spectra of calcium acquired from the CaO sample using MA-LIBS and LIBS. The gated delay time was 2 μs and the gated width was 600 μs. The laser energy was set at 5 mJ and the microwave input power was 400 W. The spectra were accumulated for the duration of 10 laser shots. The laser beam focused on a new point of the moving sample surface to avoid shot-to-shot fluctuation. For a comparison between the MA-LIBS and LIBS cases, the experimental conditions were the same. Figure 3(a) shows that the Ca ionic lines at 393.3 nm and 396.8 nm can be clearly

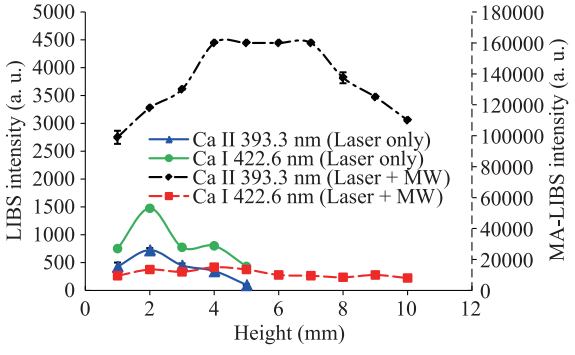

Fig. 2 Spatial distribution of Ca II 393.3 nm and Ca I 422.6 nm taken from the calcium oxide sample by using LIBS with and without microwave.

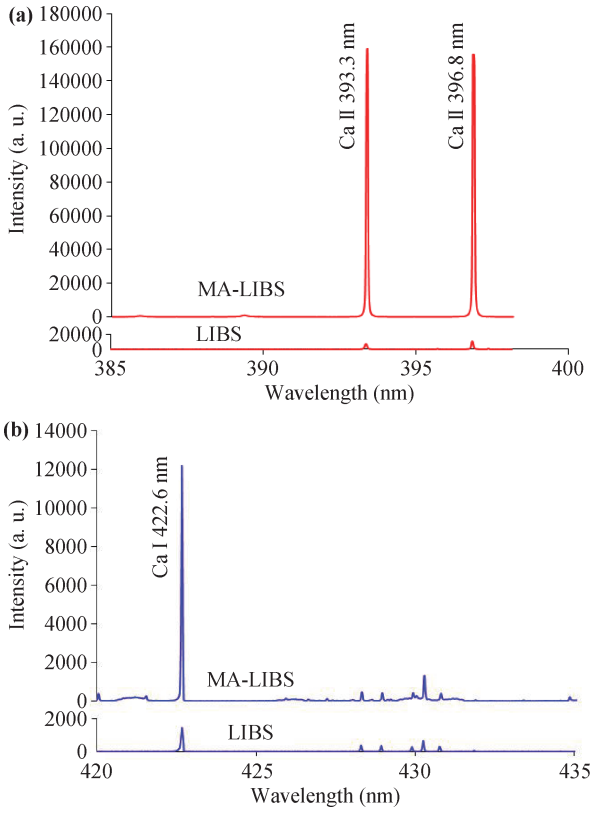

Fig. 3 Emission spectra of **(a)** Ca II at 393.3 nm and 396.8 nm, and **(b)** Ca I 422.6 nm taken from the calcium oxide sample by using LIBS with microwave and without microwave.

observed with very low background emission intensity both in the MA-LIBS and the LIBS spectra. It must be noted that, compared to LIBS, a significant intensity enhancement was obtained for the Ca ions at 393.3 nm and 396.8 nm when the MWs were employed. The enhancement factor for the Ca II 393.3 nm line is approximately 200 times; this was defined as the ratio between the MA-LIBS intensity and the LIBS intensity after subtracting the background emission. A different result was obtained for the case of the neutral emission intensity of Ca, as shown in Fig. 3(b). Namely, the enhancement factor for the Ca neutral emission intensity at 422.6 nm is significantly lower (approximately 10 times higher intensity achieved by MA-LIBS than by LIBS). The background emission is almost the same for LIBS with and without MWs, which suggests that the signal-to-background ratio (S/B ratio) is effectively enhanced when the MWs were applied. The mechanism of laser plasma enhancement by using MWs coupled with a loop antenna can be described as follows: a laser plasma is generated by a pulsed laser on a sample target near the center of the antenna, where a locally intensified electromagnetic field is produced. After several microseconds of plasma generation, the electron density of the laser plasma decreases,

especially at the outer layer of the plasma region, and the electrons absorb the MW radiation. The electrons are then accelerated and provide kinetic energy to excite the atoms and ions by multiple collisions between electrons–atoms and electrons–ions. The plasma emission can be sustained for a long time because of the long MW duration, from several hundreds of microseconds to milliseconds. As a result, the plasma emission intensity is enhanced owing to the increased integration time. The interaction between laser plasma and MWs via a charged species like electrons is consistent with the observation of the enhancement factor difference between Ca ions and atoms. Because of the Coulombic interaction, the kinetic energy can be more effectively transferred to the ions than to the neutral atoms. It must also be noted that an experiment using DP-LIBS and LIBS reported in our previous work [22] achieved a 25-fold signal intensity enhancement for DP-LIBS compared to LIBS in a Gd_2O_3 sample. This enhancement factor for DP-LIBS is significantly lower than the present result, namely, an enhancement factor of approximately 200 achieved by MA-LIBS in a CaO sample. This could be attributed to the longer lifetime of plasma emission in MA-LIBS, which results in a larger integration time compared to that of DP-LIBS. As a result, the total emission intensity in MA-LIBS is much higher than in DP-LIBS. To determine the cause of the emission intensity enhancement in the MA-LIBS method, the time-resolved emission of plasma was observed.

Figure 4 shows the emission intensity of the Ca II 393.3 nm and Ca I 422.6 nm lines as a function of delay time. The plasma emission was measured with delays of 0–5 μs after the end of the YAG laser irradiation. We observe that in the MA-LIBS case, the emission intensities for both Ca ions and Ca atoms exhibit long lifetimes of approximately 500 μs. The intensity of ionic Ca sharply increases with time to form a peak at approximately 10 μs and subsequently decreases; the intensity of Ca I reaches a peak at 10 μs. It must be noted that the intensity enhancement of Ca II is much higher than that of Ca I. At 5 μs, the MW radiation has been effectively absorbed by the laser plasma, enhancing the plasma emission as described above. The optimum intensity enhancement in the case of MA-LIBS occurs at 10 μs, which may indicate the delay time for which the absorption of the MWs by the laser plasma is optimum. Compared to the case of LIBS, which has a short plasma emission lifetime of approximately 50 μs, the emission obtained with MA-LIBS has considerably longer lifetime and higher emission intensity. As a consequence of the prolonged plasma lifetime and higher time-resolved emission intensity, the integrated emission intensity of Ca is enhanced. The results verified that the MW radiation significantly contributes to the enhancement of the laser-induced plasma emission.

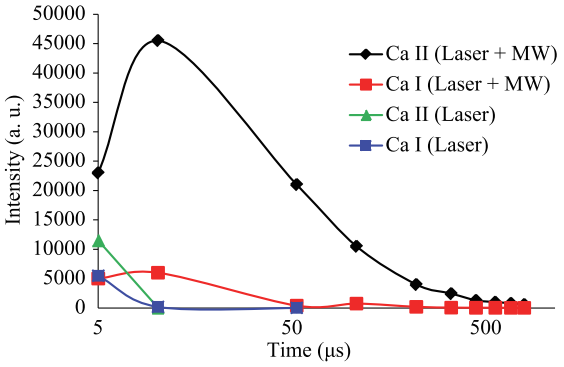

Fig. 4 Time-resolved emission profiles of Ca II 393.3 nm and Ca I 422.6 nm taken from the calcium oxide sample by using LIBS with and without microwave.

To understand the role of MWs in the enhancement of laser plasma emission, the plasma temperature and electron density in the laser plasma with and without MWs were also investigated. Selected lines and the corresponding spectroscopic data from the NIST database were used to determine the plasma temperature and electron density [23]. The lines of Ca II 315.9 nm, Ca II 317.9 nm, Ca II 318.1 nm, Ca II 370.6 nm, Ca II 393.4 nm, and Ca II 396.8 nm were employed to calculate the plasma temperature. These lines and their spectroscopic parameters, obtained from the NIST atomic database, are shown in Table 1.

To determine the plasma temperature, we assume that local thermodynamic equilibrium (LTE) is achieved [24, 25]. Examples of the Boltzmann plots of selected lines acquired with MA-LIBS and LIBS at 10 μs delay time are shown in Fig. 5(a). The slope of the curve yields a plasma temperature of approximately 10 900 K for the MA-LIBS and 9300 K for the LIBS data. The increased plasma temperature in the MA-LIBS case may be due to the effect of reheating by MW radiation, as in the case of pulsed-LIBS [26]. The introduction of the MWs into the laser plasma accelerates the electrons. Thus, the multiple collisions of electrons increase, resulting in the increase of plasma temperature. Figure 5(b) shows the

Table 1 Wavelength, upper level energy, upper level degeneracy, and transition probability for the ionic Ca emission lines used in this study.

Elements	Wavelength (nm)	Upper level energy (eV)	Upper level degeneracy	Transition probability (s^{-1})
Ca II	315.9	7.0472	4	3.1×10^8
Ca II	317.9	7.0496	6	3.6×10^8
Ca II	318.1	7.0471	4	5.8×10^7
Ca II	370.6	6.4679	2	8.8×10^7
Ca II	373.7	6.4679	2	1.7×10^8
Ca II	393.4	3.1509	4	1.5×10^8
Ca II	396.8	3.1233	2	1.4×10^8

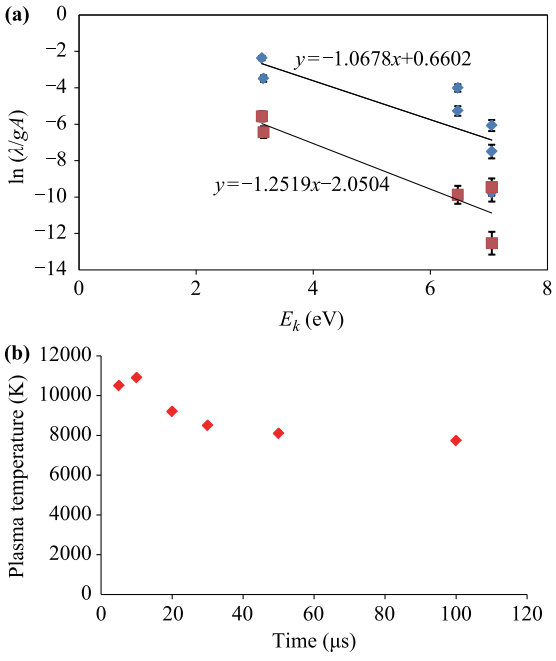

Fig. 5 **(a)** Boltzmann plot made from the analysis of Ca II lines, considering the intensities at 0.6 kPa of argon surrounding gas. The continuous line represents the result of a linear best fit. **(b)** Plasma temperature dependence of MA-LIBS on a delay time.

estimated plasma temperature in the MA-LIBS data as a function of delay time. The time duration of each point plotted in the graph is 5 μs. At 5 μs, the plasma temperature is 10 500 K; it increases to 10 900 K at 10 μs, and slowly decreases to approximately 7700 K at 100 μs. We assume that the high temperature at the initial plasma emission is due to the high electron density in the plasma region. With increasing time, the electron density decreases while the MWs continue supplying electromagnetic radiation in the plasma region, resulting in multiple collisions between electrons, atoms, and ions. The increase in plasma temperature is attributed to the MW duration. Namely, multiple electron collisions in the MW-assisted laser plasma occur continuously while the MW radiation is applied in the laser plasma region.

The high plasma temperature and long lifetime of the plasma emission observed in the MW-assisted laser plasma are due to the influence of MWs. The increased plasma temperature is attributed to the MW duration. Namely, multiple electron collisions in the MW-assisted laser plasma occur continuously while the MW radiation is applied in the laser plasma region.

The electron density of the laser plasma obtained with and without MWs was also investigated. The full width at half maximum (FWHM) of the line, $\Delta\lambda_{1/2}$, is related to the electron density N_e by the expression [27]:

$$\Delta\lambda_{1/2} = 2w\left(\frac{N_e}{10^{16}}\right) + 0.35A\left(\frac{N_e}{10^{16}}\right)^{\frac{1}{4}} \times x(1-1.2N_D^{-1/3})w\left(\frac{N_e}{10^{16}}\right), \quad (1)$$

where w is the electron impact width parameter, A the ion broadening parameter, and N_D the number of particles in the Debye sphere. For a plasma in LTE, Stark broadening is predominantly determined by the electron impact. Because the perturbations caused by ions are negligible compared with those of electrons, the electron density related to the FWHM of the Stark-broadened line $\Delta\lambda_{1/2}$ is described by the following equation [25]:

$$\Delta\lambda_{1/2} = 2w\left(\frac{N_e}{10^{16}}\right), \quad (2)$$

where N_e is the electron number density (cm^{-3}), w is the electron impact width parameter. The measured FWHM is then corrected by subtracting the contribution of the instrumental line broadening (0.05 nm). By using the Ca II 396.8 nm line and Eqs. (1) and (2), we estimated that the electron densities of the laser plasma induced at 0.6 kPa with and without MWs were 1.5×10^{18} cm^{-3} and 7.6×10^{17} cm^{-3}, respectively. From the known electron density and plasma temperature, we can confirm that the LTE assumption is valid by applying the McWhirter criterion, which provides the lower limit of the electron density [28]:

$$Ne \geq 1.6x10^{12}Te^{1/2}\Delta E^3, \quad (3)$$

where ΔE (eV) is the largest energy transition for which the condition holds and Te(K) is the plasma temperature. In this work, we used $\Delta E = 3.9$ eV for Ca and $T =$ 10 900 K, which is the highest temperature obtained by MA-LIBS. Thus, the lower limit of the electron density is approximately 9.9×10^{15} cm^{-3}. In both MA-LIBS and LIBS, the electron density in the plasma is much higher than 9.9×10^{15} cm^{-3}. Thus, the McWhirter criterion is fulfilled, verifying that the plasma at 5 mm from the sample surface was in LTE conditions.

4 Conclusions

We conducted a study on the effect of MW radiation on the enhancement of plasma emission in LIBS. In this work, MWs were introduced into a laser plasma through a loop antenna to enhance the LIBS emission. The results revealed that the optical emission intensity, plasma lifetime, electron temperature, and density were strongly influenced by the MWs. When the MWs were injected, the lifetime of plasma emission obtained by LIBS (approximately 50 μs) was extended to approximately 500

μs throughout the MW duration, the LIBS plasma temperature increased from 9300 K to 10 900 K, the electron density from 7.6×10^{17} cm^{-3} to 1.5×10^{18} cm^{-3}, and the plasma size expanded to 15 mm. As a consequence of these phenomena, the plasma emission can effectively be enhanced by using MWs and the emission intensity of Ca achieved by LIBS was increased by approximately 200 times. The final goal of the proposed method is its practical application (remote and in-situ analysis) in solid material analysis. The MA-LIBS method using a loop antenna is very suitable for practical applications because the antenna is very flexible and can access the sample by using a fiber system. Thus, it is highly applicable to material analysis in the field. In contrast, previously proposed MA-LIBS methods required waveguides and MW cavities, which is inconvenient for practical applications because the sample must be placed in a special chamber connected to the MW source.

References and notes

1. D. A. Cremers and L. J. Radziemski, Handbook of Laser-Induced Breakdown Spectroscopy, Chichester: Wiley, 2006
2. V. Miziolek, Palleschi, and I. Schechter (Eds.), Laser Induced Breakdown Spectroscopy, Cambridge: Cambridge University Press, 2006
3. Z. Wang, T. B. Yuan, Z. Y. Hou, W. D. Zhou, J. D. Lu, H. B. Ding, and X. Y. Zeng, Laser-induced breakdown spectroscopy in China, *Front. Phys.* 9(4), 419 (2014)
4. R. T. Wainner, R. S. Harmon, A. W. Miziolek, K. L. McNesby, and P. D. French, Analysis of environmental lead contamination: comparison of LIBS field and laboratory instruments, *Spectrochim. Acta B* 56(6), 777 (2001)
5. M. Z. Martin, N. Labbé, N. André, R. Harris, M. Ebinger, S. D. Wullschleger, and A. A. Vass, High resolution applications of laser-induced breakdown spectroscopy for environmental and forensic applications, *Spectrochim. Acta B* 62(12), 1426 (2007)
6. R. Noll, H. Bette, A. Brysch, M. Kraushaar, I. Mönch, L. Peter, and V. Sturm, Laser-induced breakdown spectrometry-applications for production control and quality assurance in the steel industry, *Spectrochim. Acta B* 56(6), 637 (2001)
7. M. O. Vieitez, J. Hedberg, O. Launila, and L. Berg, Elemental analysis of steel scrap metals and minerals by laser-induced breakdown spectroscopy, *Spectrochim. Acta B* 60(7-8), 920 (2005)
8. Z. B. Ni, X. L. Chen, H. B. Fu, J. G. Wang, and F. Z. Dong, Study on quantitative analysis of slag based on spectral normalization of laser-induced plasma image, *Front. Phys.* 9(4), 439 (2014)
9. A. I. Whitehouse, J. Young, I. M. Botheroyd, S. Lawson, C. P. Evans, and J. Wright, Remote material analysis of nuclear power station steam generator tubes by laser-induced breakdown spectroscopy, *Spectrochim. Acta B* 56(6), 821 (2001)
10. M. F. Bustamante, C. A. Rinaldi, and J. C. Ferrero, Laser induced breakdown spectroscopy characterization of Ca in a soil depth profile, *Spectrochim. Acta B* 57(2), 303 (2002)
11. P. Maravelaki-Kalaitzaki, D. Anglos, V. Kilikoglou, and V. Zafiropulos, Compositional characterization of encrustation on marble with laser induced breakdown spectroscopy, *Spectrochim. Acta B* 56(6), 887 (2001)
12. D. Body and B. L. Chadwick, Simultaneous elemental analysis system using laser induced breakdown spectroscopy, *Rev. Sci. Instrum.* 72(3), 1625 (2001)
13. J. Uebbing, J. Brust, W. Sdorra, F. Leis, and K. Niemax, Reheating of a laser-produced plasma by a second pulse laser, *Appl. Spectrosc.* 45(9), 1419 (1991)
14. V. I. Babushok, J. L. Jr DeLucia, C. A. Gottfried, C. A. Munson, and A. W. Miziolek, Double pulse laser ablation and plasma: Laser induced breakdown spectroscopy signal enhancement, *Spectrochim. Acta B* 61(9), 999 (2006)
15. F. F. Chen, X. J. Su, and W. D. Zhou, Effect of parameters on Si plasma emission in collinear double-pulse laser-induced breakdown spectroscopy, *Front. Phys.* 10(5), 104207 (2015)
16. R. Sattmann, V. Sturm, and R. Noll, Laser-induced breakdown spectroscopy of steel samples using multiple Q-switch Nd:YAG laser pulses, *J. Phys. D* 28(10), 2181 (1995)
17. Envimetrics, LAMPS Unit Manual, 2009
18. Y. Liu, M. Baudelet, and M. Richardson, Elemental analysis by microwave-assisted laser-induced breakdown spectroscopy: Evaluation on ceramics, *J. Anal. At. Spectrom.* 25(8), 1316 (2010)
19. B. Kearton and Y. Mattley, Laser-induced breakdown spectroscopy: Sparking new applications, *Nat. Photonics* 2(9), 537 (2008)
20. Y. Liu, B. Bousquet, M. Baudelet, and M. Richardson, Improvement of the sensitivity for the measurement of copper concentrations in soil by microwave-assisted laser-induced breakdown spectroscopy, *Spectrochim. Acta B* 73, 89 (2012)
21. Y. Ikeda, A. Moon, and M. Kaneko, Development of microwave-enhanced spark-induced breakdown spectroscopy, *Appl. Opt.* 49(13), C95 (2010)
22. M. Oba, Y. Maruyama, K. Akaoka, M. Miyabe, and I. Wakaida, Double-pulse LIBS of gadolinium oxide ablated by a femto- and nano-second laser pulses, *Appl. Phys. A* 101(3), 545 (2010)
23. http://physics.nist.gov/PhysRefData/ASD/lines_form.html
24. V. K. Unnikrishnan, K. Alti, V. B. Kartha, C. Santhosh, G. P. Gupta, and B. M. Suri, Measurements of plasma temperature and electron density in laser-induced copper plasma by time-resolved spectroscopy of neutral atom and ion emissions, *Pramana-J. Phys.* 74(6), 983 (2010)

25. J. Zalach and St. Franke, Interative Boltzmann plot method for temperature and pressure determination in a xenon high pressure discharge lamp, *J. Appl. Phys.* 113, 043303 (2013)

26. A. De Giacomo, M. Dell'Aglio, D. Bruno, R. Gaudiuso, and O. De Pascale, Experimental and theoretical comparison of single-pulse and double-pulse laser induced breakdown spectroscopy on metallic samples, *Spectrochim. Acta B* 63(7), 805 (2008)

27. S. S. Harilal, C. V. Bindhu, R. C. Issac, V. P. N. Nampoori, and C. P. G. Vallabhan, Electron density and temperature measurements in a laser produced carbon plasma, *J. Appl. Phys.* 82(5), 2140 (1997)

28. R. W. P. McWhirter, Spectral Intensities, in: Plasma Diagnostic Techniques, edited by R. H. Huddlestone and S. L. Leonard, New York: Academic, 1965